XLIII CILAMCE
21–25, November, 2022
FOZ DO IGUAÇU – PR – BRAZIL

Simulation of wheel defects and train unbalanced loads for smart detection based on wayside monitoring systems

C. Vale[1], D. Ribeiro[2], A. Mosleh[1], P. Montenegro[1], R. Silva[2], A. Guedes[3], M. Mohammadi[4], J. Meira[5], V. Gonçalves[4], A. Lourenço[5], A. Meixedo[1], G. Marreiros[5], R. Calçada[1]

[1]*CONSTRUCT, Faculty of Engineering, University of Porto,*
Rua Dr. Roberto Frias, 4200-456 Porto, Portugal
[2]*CONSTRUCT, School of Engineering, Polytechnic of Porto,*
Rua Dr. António Bernardino de Almeida, 4249-015 Porto, Portugal
[3]*School of Engineering, Polytechnic of Porto,*
Rua Dr. António Bernardino de Almeida, 4249-015 Porto, Portugal
[4]*Faculty of Engineering, University of Porto,*
Rua Dr. Roberto Frias, 4200-456 Porto, Portugal
[5]*GECAD, school of Engineering, Polytechnic of Porto,*
Rua Dr. António Bernardino de Almeida, 4249-015 Porto, Portugal
cvale@fe.up.pt

Abstract.

Keywords: damage identification, train-track dynamic interaction, numerical modelling, wheel flat, wheel polygonization, unbalanced loads, simulation.

1 Introduction

The rail sector plays an increasingly important role in society, and safety in traffic and maintenance costs are important aspects for railway managers and operators. Monitoring systems aim to contribute to these two aspects: safety and optimization of maintenance actions. However, current monitoring systems placed on the track, despite identifying geometric defects in the wheels, such as flats, they do not categorize them in terms of severity or identify in operation, risk situations in railway circulation, such as unbalanced loads. In this context, the research on the WAY4SafeRail project aims identifying the condition of the train wheels in operation and detecting situations of instability in railway circulation, such as unbalanced loads. This paper presents part of the research developed in the WAY4SafeRail project framework, namely the numerical simulations of wheel defects and unbalanced loads as a preliminary step of the application of Artificial Intelligence Techniques.

2 Modelling

2.1 Track model

The track is modelled in ANSYS® [1] with a multiple-layer scheme, in which the ballast, sleepers and rails are linked through elastic elements that represent the mechanical behaviour of the interface, as shown in Figure 1. The ballast mass is simulated by using discrete mass point elements, while the sleepers and rails are modelled with beam elements with the appropriate properties. The interfaces, namely the ballast and pads/fasteners, located below and above the sleepers, respectively, have been considered by using spring-dashpot elements in the three

directions. Finally, spring-dashpot elements are used to consider the foundation flexibility. The properties of the track model, including the description of the variables presented in Figure 1, are presented in [2].

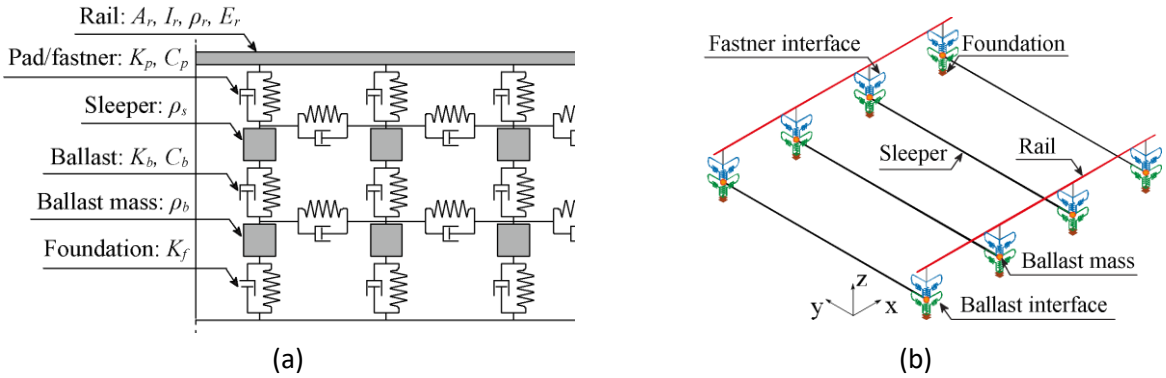

Figure 1. Numerical model of the track: (a) multi-layer representation and (b) FE model.

2.2 Vehicle model

The vehicle used in this study is a five-freight wagon of the Laagrss type, whose dynamic model is illustrated in Figure 2. The three-dimensional (3D) multibody dynamic model has been developed in ANSYS® [1] with spring-dashpot elements to simulate the suspensions in all the directions and mass point elements to represent the mass and inertial effects in the centre of gravity of each component of the cars (carbody, bogies and wheelsets). Rigid beam elements are adopted to link the aforementioned elements. The mechanical properties of the vehicle, namely stiffness and damping of the suspensions, denoted by *k* and *c* in Figure 2, and mass and rotary inertias, indicated by *m* and *I* in the same figures, can be consulted in previous works from the authors [2]. Moreover, the geometrical properties, such as longitudinal, transversal and vertical distances, referred as *a*, *b* and *h*, and nominal wheel radius and gauge, denoted by R_0 and *s*, are also available in the same reference [2]. The subscripts c_b, *b* and *w* indicate that the respective property is related to the carbody, bogies and wheelsets, respectively. However, the freight wagon is only one level of suspension, without any bogie, once the wheelset is connected directly to the carbody through the suspension.

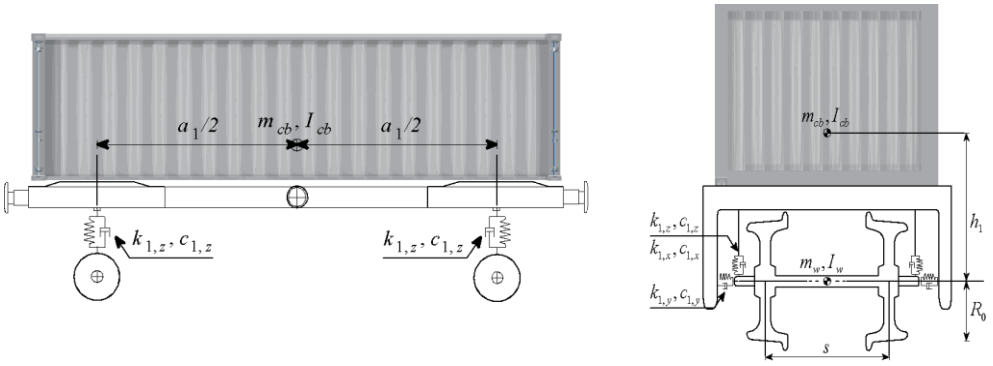

Figure 2. Dynamic model of the Laagrss freight wagon.

2.3 Track irregularity profile

Based on accurate data, power spectral density (PSD) curves are generated and artificial unevenness profiles were created in a vertical and transverse direction. To generate the rail unevenness profiles, wavelengths between 1 m to 75 m are used, which covers D1 and D2 wavelength intervals defined by the European Standard [3], with a sampling discretization of 0.01 m. More details about the generation of unevenness profiles are provided by Mosleh et al. [4].

2.4 Wheel flat modeling

Various combinations of flat wheel depth (D_w) and flat wheel length (L_w) are considered with a uniform statistical distribution. A uniform distribution U (50,100) [mm] defines the lower and upper limits of a flat wheel length, and the wheel flat depth is calculated using the following equation [5]:

$$D_w = \frac{{L_w}^2}{16R} \tag{1}$$

In which R is the radius of the wheel. The vertical profile deviation of the wheel flat is defined as:

$$Z = -\frac{D_w}{2}\left(1 - cos\frac{2\pi x}{L_w}\right).H\left(x - (2\pi R - L_w)\right),\ \ 0 \leq\ x \leq 2\pi R \tag{2}$$

where H represents the Heaviside function.

2.5 Wheel polygonization modelling

The initial wheel irregularity level due to polygonization is determined by following function [6]:

$$L_{w\theta} = 24.7\ log_{10}^{\lambda_\theta} + 8.47 \tag{3}$$

The harmonic orders θ of the polygonization are defined, so that the wavelengths λ_θ are given by

$$\lambda_\theta = \frac{2\pi R}{\theta}\ \ ,(\theta = 17 - 20) \tag{4}$$

In this study, the wavelengths corresponding to the 17 to 20 harmonic orders of a polygonalized wheel are considered with the uniform distributions U (17,20). For each wavelength, the amplitude of the sine function is obtained as

$$a_\theta = \sqrt{2}\,.\,10^{\frac{L_{w\theta}}{20}}\,.\,w_{ref} \tag{5}$$

w_{ref} is 1μm. By assigning phase angles to sinusoidal functions that are uniformly and randomly distributed between 0 and 2π, the irregularity of different wheels defined by the same spectrum is generated.

2.6 Vehicle-track interaction

The numerical vehicle-track dynamic interaction simulations are carried out with the in-house software VSI – Vehicle-Structure Interaction Analysis validated and described in detail in an authors' previous publication [7] and used in distinct applications [8, 9]. The key point of this model lies in the wheel-rail contact element connecting the two subsystems. This element governs the contact interface, more precisely the evaluation of the wheel-rail contact forces in the normal and tangential directions. After determining in each time step the position of the contact point, the algorithm computes the normal contact force through the Hertz nonlinear theory [10] and the lateral and longitudinal tangential creep forces through the USETAB routine [11]. This numerical tool is implemented in MATLAB® [12] and imports the structural matrices from both the vehicle and structure (in this case, the track) previously modeled in a finite element (FE) package, which in this study is ANSYS® [1]. Note that, although the models of both subsystems are firstly modeled separately, the VSI software links them through a fully coupled methodology. The full description of the formulation may be found in Montenegro et al. [7].

2.7 Virtual monitoring device

A virtual wayside monitoring system installed along the track to detect wheel defects and unbalanced load consists of 44 accelerometers (22 located on the right side and 22 located on the left side) depicted in Figure 3. In this

figure, the numbers 1-to-10 and 11-to-16 represent the position of the measurement points mounted on the rail between two sleepers and over the sleepers on the right side. Moreover, number 17-to-22 is the number of sensors located on the sleeper. The same numbering for sensors 23-to-44 is considered for the left side.

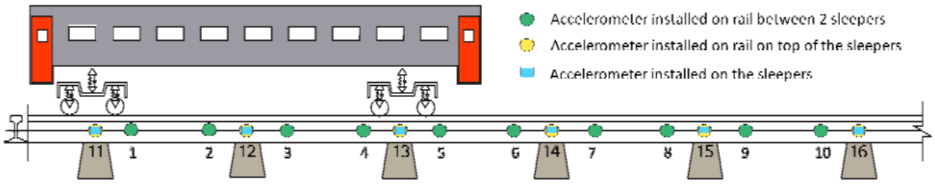

Figure 3. Virtual wayside monitoring system

Several simulations including 120 train passages with a healthy wheel are summarized in Table 1 to reproduce the rail's response at five different speeds, six loading scenarios, and four unevenness profiles generated as indicated in section 2.3. The considered loading scenarios are full, empty and half loading plus three unbalanced loading under the limits (two in the longitudinal direction and one in the transversal one).
Regarding the damaged scenarios, thirty simulations for each type of defect including wheel flat and polygonalisation as well as unbalanced load are performed with respect to five vehicles of the freight train. In terms of the sampling frequency, 10 kHz sampling frequency is used and an artificial noise (5%) is generated and added to the original numerical signal, to obtain a more similar and reliable reproduction of the rail response. In this study, three defective wheels are considered in terms of its position: the first wheel of the first vehicle on the right side, the second wheel of the third vehicle on the left side and last wheel of the fifth vehicle on the right side.

Table 1. Damaged and undamaged simulations

	Undamaged wheel	**Damaged wheel - flats**	**Damaged wheel - polygonization**	**Unbalanced loads**
Train		five freight wagon of the Laagrss type		
Number of Loading schemes	6 scenarios	1 type	1 type	1 type
Unevenness profile	4 profiles	1 profile	1 profile	1 profile
Speed range	40-120 km/h	80 km/h	80 km/h	80 km/h
Noise ratio	5%	5%	5%	5%
Defect	-	Flat lengths: 50-100 mm	17 to 20 harmonic orders	gravity centre offset, exceeding the UIC ratios
Total analysis	**120**	**30**	**30**	**30**

3 Simulation

3.1 Unbalanced load

According to the UIC code of practice for the loading and securing of goods on railway wagons [13], different unbalanced load schemes were defined for Laagrss wagon model, illustrated in Figure 4, where the cargo gravity centre is offset in longitudinal and transversal directions. The UIC code [13] defines a ratio of 2:1 between the masses per axle, and a ratio of 1.25:1 between the masses per wheel, which should not be exceeded. The balanced full load scheme presented in Figure 4a) corresponds to an evenly load distribution on the wagon with two containers with 15 tons each, without exceeding the maximum mass per axle. The unbalanced load schemes correspond to a longitudinal (Figure 4b) and a transversal (Figure 4c) offset of the cargo gravity centre, which exceeds the UIC code ratios.

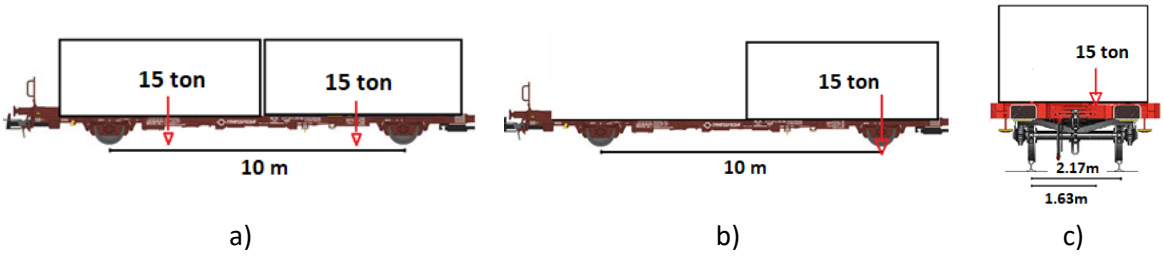

Figure 4. Laagrss load schemes: a) balanced full load; b) longitudinal unbalanced load: c) transversal unbalanced load.

Figure 5 depicts time-series examples of accelerations evaluated from position 1 due to a five-freight-wagon passage at 80km/h with the balanced and unbalanced loads schemes presented in Figure 4. All time-series were filtered based on a low-pass Chebyshev type II digital filter with a cut-off frequency equal to 500 Hz. The results consider the unbalanced load schemes only for the first wagon and the rest were set with the full load scheme. Figure 5a shows the comparison between balanced and longitudinal unbalanced scenarios, while Figure 5b shows the comparison between left and right rail considering a transversal unbalanced load scheme. The results show a difference in terms of peak acceleration values during the first wagon passage, where the unbalanced loads are present. In the case of the transversal unbalanced load, the acceleration peak values are higher for the right rail than left rail, consequence of the load asymmetry.

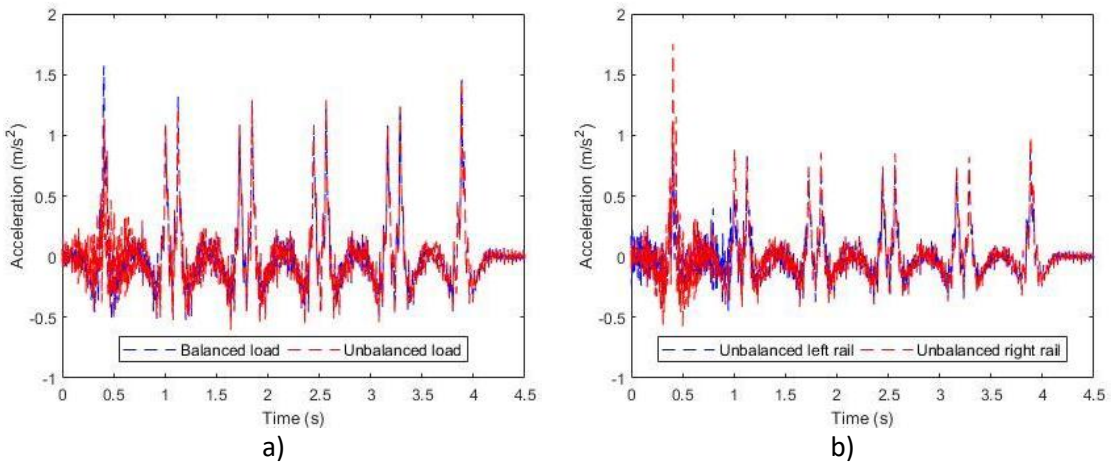

Figure 5. Acceleration response for: a) longitudinal balanced/unbalanced load; b) transversal unbalanced load.

3.2 Wheel flats

Wheel flats induce high impact loads with relevance on safety of vehicle in operation as they can contribute for broken axles, hot axle boxes, damaged rolling bearings and wheels [14]. Several time-series samples are simulated and divided according to two main groups. The first group is the passage of a healthy wheel, while the second group is the passage of a train with a defective wheel. The assumptions for damage and healthy simulations, including the total number of analyses for each group, are summarized in Table 1.

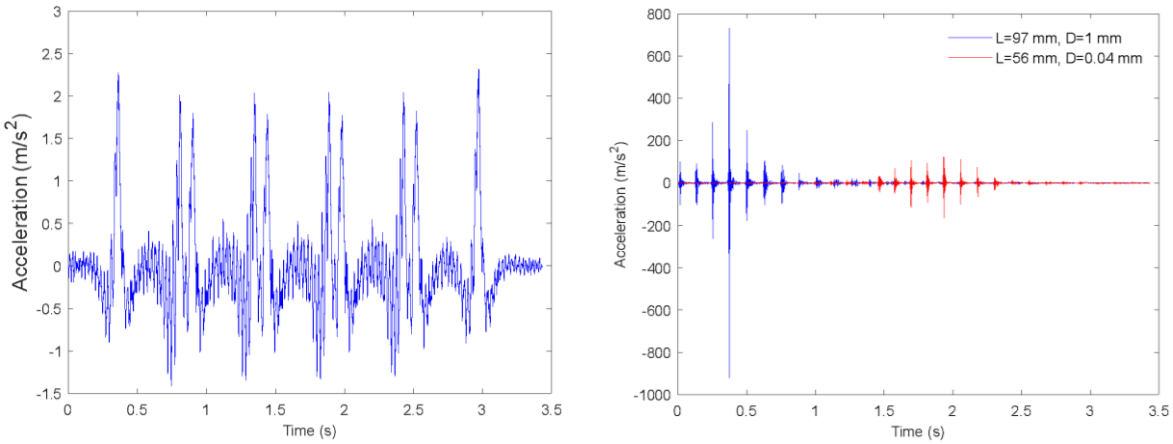

(a) (b)

Figure 6. Time-series signal corresponding to the (a): healthy wheel, (b) damaged wheel

Figure 6 depicts time-series examples of acceleration evaluated from position 1 (presented in Figure 3) due to the passage of freight vehicle considering healthy and damaged wheels. All time-series are filtered based on a low-pass Chebyshev type II digital filter with a cut-off frequency of 500 Hz. The effect of two types of wheel flat properties is shown in Figure 6b. The acceleration variation for the healthy wheel passage changes between -1.5 to 3 m/s^2 (Figure 6a). Severe wheel flat with L=97 mm, located in the first wheel of the first vehicle on the right side, generates a higher amplitude in the signal (-1000 to 800 m/s^2), while the amplitude variation for the second wheel of the third vehicle on the left side with L=56 mm is between -200 to 200 m/s^2

3.3 Wheel polygonization

Different locations of polygonal wheels are considered in the numerical simulations of the freight wagon passages. A set of five wagons is assumed where polygonal damage is reproduced on the wheels of the 1st wagon, 3rd wagon, and 5th wagon, as illustrated in Figure 7(a) for the example of the 3rd wagon. Figure 7(b) shows the comparison of the measurement of the rail acceleration in the time domain against the load imposed by the train with and without polygonal damage on the wheels, where a slight difference is visible when compared with other types of phenomena of peripheral circular irregularity of the wheel, namely flat wheels as presented in section 3.2. Due to the geometry of the polygonal damage, which does not present a marked unevenness between the successive perimetric areas of the wheel, a significant impact load is not produced on the track, and therefore, it is possible to expect response values that are not very different from the situations with and without damage.

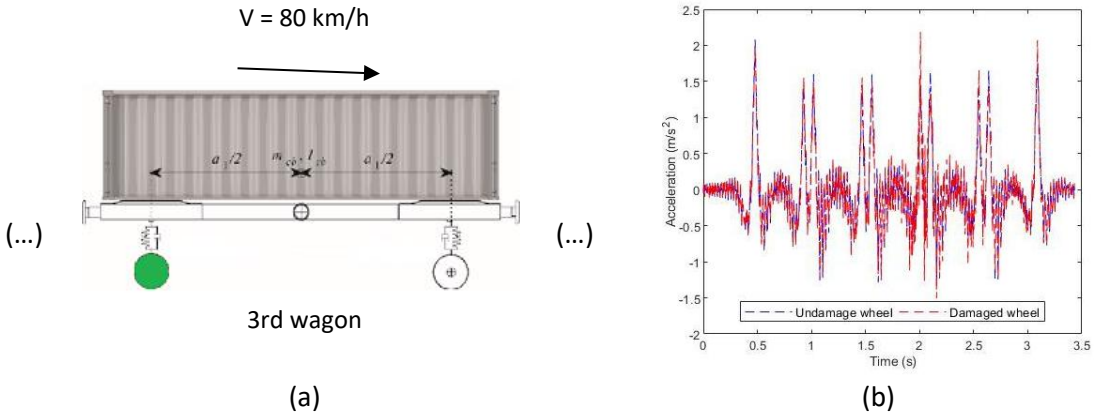

(a) (b)

Figure 7. (a) location of defective wheels (b) Acceleration response for undamaged and damaged scenario on the 2nd wheel of the 1st wagon.

4 Conclusions and future developments

This article presented several simulation results from a virtual wayside monitoring system for the passage of a freight vehicle with specific damages related to wheel defects, particularly flats and polygonization, as well as unbalanced vertical axle loads. In future developments of this work, and based on the simulation results, the authors intend to propose an automatic fault detection and classification methodology that can accurately identify these abnormal situations that can put in risk the running safety of the operating trains. The proposed methodologies will be based on Artificial Intelligence (AI) algorithms using two distinct unsupervised approaches. The first approach is based on a strategy that comprises [15]: i) feature extraction from the measured data (autoregressive model coefficients, Wavelet coefficients, etc.); ii) feature normalization to remove the influence of the ambient and operation effects; iii) feature fusion; and iv) feature classification. The second approach is directly applied to the time domain records and involves the application of two anomaly detection methods capable of dealing with data streams. The first method, denominated as xStrream [16], is a density-based technique scoring the data points relative to the density region around each point. Then, the second method, which identifies volatility in streams [17], takes the output of the first method to find gaps in the data sensors where those gaps represent the occurrence of anomalies.

Acknowledgements. This paper is a result of project WAY4SafeRail- WAYside monitoring system FOR SAFE RAIL transportation, with reference NORTE-01-0247-FEDER-069595, co-funded by the European Regional Development Fund (ERDF), through the North Portugal Regional Operational Programme (NORTE2020), under the PORTUGAL 2020 Partnership Agreement.

Authorship statement. The authors hereby confirm that they are the sole liable persons responsible for the authorship of this work, and that all material that has been herein included as part of the present paper is either the authorship of the authors, or has the permission of the owners to be included here.

References

[1] ANSYS®. ANSYS Inc, Canonsburg, PA, USA, 2018.
[2] Mosleh, A., P. Costa, and R. Calçada, *A new strategy to estimate static loads for the dynamic weighing in motion of railway vehicles.* Proceedings of the Institution of Mechanical Engineers, Part F: Journal of Rail and Rapid Transit, 2020. **234**(2): p. 183-200.
[3] EUROPEAN STANDARD, Railway applications - Track - Track geometry quality - Part 2: Measuring systems - Track recording vehicles (EN 13848-2). 2006, Brussels: EUROPEAN COMMITTEE FOR STANDARDIZATION.
[4] Mosleh, A., P. Costa, and R. Calçada, A new strategy to estimate static loads for the dynamic weighing in motion of railway vehicles. Proceedings of the Institution of Mechanical Engineers, Part F: Journal of Rail and Rapid Transit, 2020. 234(2): p. 183-200.
[5] Zhai, W., et al., *Dynamic effects of vehicles on tracks in the case of raising train speeds.* Proceedings of the Institution of Mechanical Engineers, Part F: Journal of Rail and Rapid Transit, 2001. **215**(2): p. 125-135.
[6] Johansson, J. and C. Andersson, *Out-of-round railway wheels—a study of wheel polygonalization through simulation of threedimensional wheel–rail interaction and wear.* Vehicle system dynamic, 2005. **43**(8): p. 539–559.
[7] Montenegro PA, Neves SGM, Calçada R, Tanabe M, Sogabe M, Wheel-rail contact formulation for analyzing the lateral train-structure dynamic interaction, Computers & Structures 2015; 152: 200-214. DOI:10.1016/j.compstruc.2015.01.004.
[8] Mosleh A, Montenegro P, Costa P, Caçada R, Railway Vehicle Wheel Flat Detection with Multiple Records Using Spectral Kurtosis Analysis, Applied Sciences 2021; 11 (9): 4002. DOI:10.3390/app11094002.
[9] Montenegro PA, Heleno R, Carvalho H, Calçada R, Baker CJ, A comparative study on the running safety of trains subjected to crosswinds simulated with different wind models, Journal of Wind Engineering and Industrial Aerodynamics 2020; 207: 104398. DOI:10.1016/j.jweia.2020.104398.
[10] Hertz H, Ueber die Berührung fester elastischer Körper [On the contact of elastic solids], Journal für die reine und angewandte Mathematik 1882; 92: 156-171.
[11] Kalker J. Book of tables for the Hertzian creep-force law. Budapest, Hungary., 1996.
[12] MATLAB®. Release R2018a, The MathWorks Inc., Natick, MA, USA, 2018.

[13] UIC. Code of practice for the loading and securing of goods on railway wagons. Paris. 2022
[14] Vale C. Wheel Flats in the Dynamic Behavior of Ballasted and Slab Railway Tracks. *Applied Sciences*. 2021; 11(15):7127. https://doi.org/10.3390/app11157127
[15] A. Meixedo, J. Santos, D. Ribeiro, R. Calçada, M. Todd (2021) – "Damage detection in railway bridges using traffic-induced dynamic responses", Engineering Structures, Volume 238, 112189, DOI: 10.1016/j.engstruct.2021.112189.
[16] Manzoor, Emaad, Hemank Lamba, and Leman Akoglu. "xstream: Outlier detection in feature-evolving data streams." Proceedings of the 24th ACM SIGKDD International Conference on Knowledge Discovery & Data Mining. 2018.
[17] Yilmaz, Selim F., and Suleyman S. Kozat. "PySAD: a streaming anomaly detection framework in Python." arXiv preprint arXiv:2009.02572 (2020).